A&A 407, 289–301 (2003)
DOI: 10.1051/0004-6361:20030723

Astronomy & Astrophysics

The evolution of lithium depletion in young open clusters: NGC 6475⋆

P. Sestito[1], S. Randich[2], J.-C. Mermilliod[3], and R. Pallavicini[4]

[1] Dipartimento di Astronomia, Università di Firenze, Largo E. Fermi 5, 50125 Firenze, Italy
[2] INAF/Osservatorio Astrofisico di Arcetri, Largo E. Fermi 5, 50125 Firenze, Italy
[3] Institut d' Astronomie, Université de Lausanne, 1290, Chavannes–des–Bois, Switzerland
[4] INAF/Osservatorio Astronomico di Palermo, Piazza del Parlamento 1, 90134 Palermo, Italy

Received 27 February 2003 / Accepted 12 May 2003

Abstract. We have carried out a high resolution spectroscopic survey of the 220–250 Myr old cluster NGC 6475: our main purpose is to investigate Li evolution during the early stages of the Main Sequence. We have determined Li abundances for 33 late F to K–type X–ray selected cluster candidates, extending the samples already available in the literature; for part of the stars we obtained radial and rotational velocities, allowing us to confirm the membership and to check for binarity. We also estimated the cluster metallicity which turned out to be over–solar ([Fe/H] = +0.14 ± 0.06). Our Li analysis evidenced that (i) late F–type stars ($T_{\rm eff} \gtrsim 6000$ K) undergo a very small amount of Li depletion during the early phases on the ZAMS; (ii) G–type stars ($6000 \gtrsim T_{\rm eff} \gtrsim 5500$ K) instead do deplete lithium soon after arrival on the ZAMS. Whereas this result is not new, we show that the time scale for Li depletion in these stars is almost constant between 100 and 600 Myr; (iii) we confirm that the spread observed in early K–type stars in younger clusters has converged by 220 Myr. No constraints can be put on later–type stars. (iv) Finally, we investigate the effect of metallicity on Li depletion by comparing NGC 6475 with the similar age cluster M 34, but we show that the issue remains open, given the uncertain metallicity of the latter cluster. By using the combined NGC 6475+M 34 sample together with the Hyades and the Pleiades, we compare quantitatively Li evolution from the ZAMS to 600 Myr with theoretical predictions of standard models.

Key words. stars: abundances – stars: evolution – open clusters and associations: individual: NGC 6475

1. Introduction

Studies of lithium abundances in stars are very important since Li survives only in the outermost layers of a star, due to its low burning temperature: for this reason, Li is a good tracer of mixing mechanisms occurring in stellar interiors during the various phases of stellar evolution. Several Li surveys in open clusters have been carried out during the last two decades, in order to investigate Li destruction processes and mixing mechanisms, and their dependence on age, mass and chemical composition. The resulting empirical picture has evidenced several features that cannot be explained with standard theoretical models that include only convection as a mixing mechanism (see e.g. the review by Pasquini 2000 and references therein).

Standard models predict a certain amount of depletion during Pre–Main Sequence (PMS) evolution of solar–type stars (e.g. D' Antona & Mazzitelli 1994) and no depletion at all after arrival on the Zero–Age Main Sequence (ZAMS). The predicted PMS Li depletion increases as mass decreases while the predicted Main Sequence (MS) depletion remains small in all cases, apart from the coolest stars; moreover Li depletion should depend only on age, chemical composition and mass (or effective temperature), i.e. stars with the same mass in a given cluster should all have the same Li abundance. As far as the Li–metallicity relationship is concerned, standard models predict that increased metal abundances should lead to a significant increase of Li depletion during PMS contraction for stars cooler than ~6000 K (e.g. Chaboyer et al. 1995; Swenson et al. 1994): this is due to the fact that the gas opacity grows up in stars with a higher iron content, thus the depth of the convective zone (CZ) increases leading to a large amount of Li depletion. It is worth of mention that also oxygen, as well as other α elements, largely contributes to affect the opacity values and thus the depth of the CZ (Piau & Turck–Chièze 2002).

The predictions of standard models are in contrast with observational results. Namely, focusing on the evolution of Li up

Send offprint requests to: P. Sestito,
e-mail: sestito@arcetri.astro.it

⋆ Based on observations collected at the European Southern Observatory.

to the Hyades age (~600 Myr), observations of very young clusters (ages 30–50 Myr) show that solar analogs undergo very little (if any) Li depletion during the PMS (e.g. Martín & Montes 1997; Randich et al. 1997); on the other hand, the comparison of clusters of different ages clearly shows that these stars do deplete Li while on the MS. Furthermore, the star–to–star scatter in Li abundance seen in young clusters for stars cooler than ~5500 K (e.g. Soderblom et al. 1993 – hereafter S93; García López et al. 1994; Jones et al. 1996; Randich et al. 1998) is clearly in contrast with standard model predictions; this dispersion is already present at arrival on the ZAMS and has disappeared by the age of the Hyades (~600–700 Myr, Thorburn et al. 1993). Based on the observed Li–rotation relationship (S93), and specifically on the fact that rapid rotators in young clusters have on average higher Li abundances than slow rotators, the most commonly accepted explanation for the scatter is that Li depletion is connected to rotationally driven mixing and angular momentum transport. Note however that slow rotators in young clusters can have either high or low Li abundances, as showed by Randich et al. (1998) for α Persei, and that the Li–rotation relationship breaks down for the coolest stars ($T_{\rm eff} \lesssim 4500$ K, García López et al. 1994).

Finally, the fact that no Li depletion–metallicity relationship has so far been convincingly demonstrated (see for example Jeffries & James 1999), at least for $T_{\rm eff} \gtrsim 4700$ K, appears in contrast with model predictions.

In summary, the question remains which mechanism(s) drives or inhibits Li depletion in stars of different masses during the PMS and MS phases.

In order to put additional empirical constraints on early–MS Li depletion processes, it is necessary to enlarge the database of Li observations in young clusters; for this reason, we carried out a survey of NGC 6475, a well populated Southern hemisphere cluster, with reported over–solar metallicity. NGC 6475 is a very good target, since its age of ~220 Myr (Meynet et al. 1993) is intermediate between those of the Pleiades and of the Hyades and it is the closest and most compact open cluster at that age (distance ~250 pc); the estimated spectroscopic iron abundance is [Fe/H] = +0.11 ± 0.034 and the reddening $E(B-V) = 0.06$ (James & Jeffries 1997 – hereafter JJ97). Li data for this cluster allow us to investigate early–MS Li depletion and its time scale for solar–type and lower mass stars, as well as, to some extent, the dependence of Li depletion on metallicity by comparing NGC 6475 to M 34 (NGC 1039), surveyed by Jones et al. (1997). The latter cluster is about co–eval to NGC 6475 (~250 Myr, Jones & Prosser 1996); Canterna et al. (1979) found a solar metallicity for M 34, based on multicolor ubvy photometry of two F–type stars, while a recent and more detailed high resolution spectroscopic analysis by Schuler et al. (2003) evidenced that the iron content could be over–solar ([Fe/H] = +0.07 ± 0.04). Note that the result of Schuler et al. (2003) is based on five solar–type stars; had they considered their whole sample of nine stars with $4750 \leq T_{\rm eff} \leq 6130$ K, they would have found [Fe/H] = +0.02 ± 0.02 (see the quoted reference for more details).

Previous studies of Li in NGC 6475 were carried out by JJ97 and James et al. (2000) (hereafter J00): the first one is based on an X–ray selected sample, while in the latter one an optically selected sample is studied. In this paper, we present the results of additional Li observations of NGC 6475: our data, merged with the ones of the two previous works, provide a larger and more statistically significant sample of stars to further address the issue of Li evolution between the age of Pleiades and that of the Hyades. In addition, our sample contains a few more stars of later spectral–types than the previous surveys, allowing us to get some insights on early–MS Li depletion for the coolest stars.

In Sect. 2 we describe our sample and the observations; in Sect. 3 we summarize the radial velocities and abundances analysis, while the results and a discussion are presented in Sects. 4 and 5. Finally our conclusions (Sect. 6) close the paper.

2. Observations

Our original sample includes 34 cluster candidates with $0.50 \leq (B-V)_0 \leq 1.44$, selected from the X–ray survey of Prosser et al. (1995) (hereafter P95). Target stars and photometry are listed in the first three columns of Table 1: the identification number (Col. 1) and the photometry (Cols. 2 and 3) were retrieved from P95; a reddening $E(B-V) = 0.06$ was adopted.

The observations were carried out during three runs (April 1994, April 1995 and July 1996) at the European Southern Observatory (ESO), La Silla, Chile, with the 3.6 m telescope equipped with CASPEC. During the April 1994 and April 1995 observing runs the standard echelle grating (31.6 lines mm^{-1}) with the red cross–disperser (158 lines mm^{-1}) and the short camera were used, together with ESO CCD #32 (TK512, with 512 × 512 pixels of 27 μ); the nominal resolving power was $R \sim 20\,000$ (slit aperture of 280 μm). In the July 1996 run the long camera and the ESO CCD #37 (TK1024, with 1024×1024 pixels of 24 μ) were used with a slit aperture of 200 μm, which provided a slightly larger resolving power, $R \sim 29\,000$. Exposure times ranged between 10 min and 1.5 hours resulting in S/N ratios of 50–150. For each star, the corresponding CASPEC run and exposure time are listed in Cols. 4 and 5 of Table 1.

About 80% of the stars were also observed with the CORAVEL instrument (Baranne et al. 1979) at the 1.54 m Danish telescope at ESO. Three observations were obtained through the period 1985–1995 for stars belonging to a program designed to search for faint members, and one or two measurements were obtained in April and July 1996 for stars selected from the ROSAT X–ray source catalog (P95) during the course of a long–term systematic program on cluster red dwarfs started in Chile in 1983. We mention that part of the stars of the JJ97 sample were also observed by us with CORAVEL. The CORAVEL observations allowed us to derive radial velocities and to check for binarity; for part of the stars the projected rotational velocities ($V \sin i$) were also determined.

CASPEC data reduction was performed with the package MIDAS in the ECHELLE context, following the usual steps: bias subtraction, order definition, order extraction, inter–order background subtraction, flat–fielding and wavelength calibration. Figure 1 shows examples of normalized spectra in the Li region.

Table 1. Photometry, exposure times, radial and rotational velocities and membership for target stars selected from P95.

No. P95	V	$(B-V)_0$	Observing run (CASPEC)	Exposure time [s]	RV [km s^{-1}]	N	$V \sin i$ [km s^{-1}]	Spectroscopic membership (CORAVEL)
R10A	12.99	1.04	July 1996	3600	–	–	–	No information
R14	12.06	0.60	April 1995	1200	-15.60 ± 0.24	4	6.0 ± 1.6	M
R15A	12.28	0.65	July 1996	2700	$+18.60 \pm 0.56$	1	15.0 ± 2.0	N?, SB
R16A	11.69	0.66	April 1994	720	-13.77 ± 0.34	2	5.8 ± 2.4	M
R26A	14.89	1.44	July 1996	5400	–	–	–	No information
R27	12.12	0.62	April 1994	1200	-14.98 ± 0.33	3	9.8 ± 1.3	M
R35	14.54	1.25	July 1996	4800	–	–	–	No information
R39A	12.36	0.65	April 1995	1320	-14.03 ± 0.23	4	4.5 ± 1.5	M
R42	11.83	0.57	July 1996	1800	-11.23 ± 0.43	2	14.3 ± 2.3	M, SB
R48A	14.73	1.22	July 1996	5400	–	–	–	No information
R49A	12.37	0.63	July 1996	2700	-13.90 ± 0.50	1	5.9 ± 2.8	M
R51A	12.25	0.63	April 1995	1200	-11.81 ± 1.06	1	14.3 ± 3.3	M
R53	13.40	0.84	April 1995	1800	-12.83 ± 0.56	1	3.7 ± 3.2	M
R55A	12.33	0.77	April 1995	1200	-19.58 ± 0.47	1	9.0 ± 1.8	M, SB?
R55B	11.70	0.54	July 1996	2400	-13.59 ± 0.59	4	13.7 ± 4.6	M, SB
R64	11.96	0.67	April 1994	1200	-14.44 ± 0.56	2	5.8 ± 1.8	M
R66	12.78	0.72	April 1995	1500	-15.71 ± 0.45	3	7.7 ± 1.3	M, SB2
R73A	10.95	0.51	April 1994	600	-12.56 ± 1.11	4	18.7 ± 2.2	M, SB
R79A	11.92	0.70	July 1996	1800	-15.71 ± 0.33	2	6.9 ± 1.5	M
R82	12.87	0.67	April 1995	1620	-14.69 ± 0.30	3	6.7 ± 1.5	M
R92	12.46	0.63	April 1995	1020	$+4.31 \pm 1.03$	2	8.1 ± 1.6	M, SB?
R97	12.17	0.63	April 1994	900	-13.97 ± 0.50	1	9.7 ± 1.8	M
R102	13.32	0.83	April 1995	2100	-15.97 ± 0.56	1	6.1 ± 4.3	M
R103	12.37	0.65	April 1995	1500	-13.56 ± 0.43	1	2.4 ± 2.8	M
R105	12.26	0.62	April 1994	1020	-10.22 ± 0.53	1	11.0 ± 2.0	M, SB
R109A	12.56	0.71	April 1994	1200	-6.31 ± 1.06	2	6.8 ± 3.0	M?, SB
R116	12.77	0.82	April 1995	1560	$+10.59 \pm 25.86$	3	7.5 ± 1.8	M?, SB
R123	13.17	0.79	April 1995	1800	-15.37 ± 0.54	1	9.8 ± 2.1	M
R126A	11.45	0.50	April 1994	720	–	–	–	No information
R133	12.17	0.65	April 1995	1200	-12.72 ± 16.07	3	7.5 ± 1.3	M?, SB
R135A	13.08	0.96	July 1996	3300	–	–	–	No information
R136A	11.43	0.70	July 1996	1800	-14.83 ± 0.81	1	26.2 ± 2.6	M, SB2
R137A	13.43	0.93	July 1996	3600	–	–	–	No information
R140B	12.38	0.76	July 1996	3000	-14.83 ± 0.44	1	1.9 ± 3.1	M

3. Analysis

3.1. Radial velocities and membership

The radial velocities are on the system defined by Udry et al. (1999) from high–precision radial–velocities obtained with the ELODIE spectrograph (Baranne et al. 1996). This calibration corrects for the systematic errors of the CORAVEL system. $V \sin i$ values are derived from the width of the cross–correlation function according to the calibration of Benz & Mayor (1984). Our mean results for individual stars in NGC 6475 are summarized in Cols. 6–8 of Table 1 (our sample) and Cols. 2–4 of Table 2 (JJ97 sample) which give the mean radial velocities with the errors in [km s^{-1}], the number of radial–velocity observations, and the projected rotational velocities $V \sin i$ and their errors, also in [km s^{-1}].

Results for further stars and individual observations will be discussed in a separate paper devoted to the study of NGC 6475 based on CORAVEL observations. If necessary, data used in the present paper are available from J.–C. Mermilliod.

CORAVEL radial velocities have been used in conjunction with available data, from P95 and JJ97, which are usually based on one observation, to detect spectroscopic binaries and confirm the membership of the other stars. The results are recorded in Col. 9 of Table 1 and Col. 5 of Table 2 as membership determinations and remarks on duplicity (M: member, M?: possible member, N?: doubtful member, N: non–member, SB: spectroscopic binary, SB?: possible spectroscopic binary, No information: the star has not been observed with CORAVEL). In Table 2 the identification numbers of JJ97 are used (Col. 1).

Several stars require a comment:

- R15A: it is a binary, but all three observations are positive. The membership is doubtful.
- R42: the difference between the RV of JJ97 (-16.2 km s^{-1}) and CORAVEL RV reaches 5 km s^{-1} and, according to the errors, R42 is certainly a binary.
- R55A: the only RV obtained is off the cluster mean velocity by 4 km s^{-1} and should be a binary if it is a member, as judged from it position in the CMD.
- R66: it has been declared SB2 by P95 and its radial velocity is clearly variable.

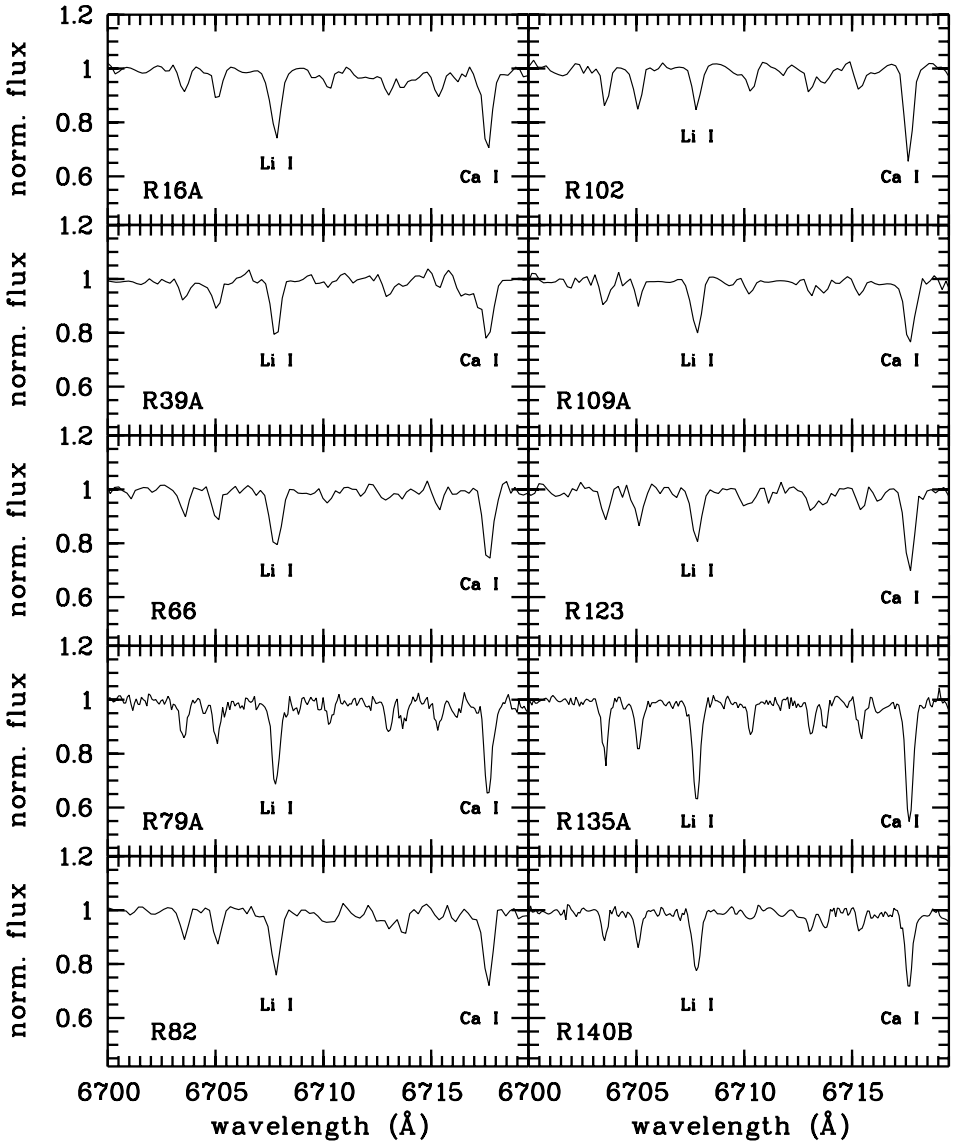

Fig. 1. Sample spectra in the Li region.

- R92: this star is either a binary or a non–member. The two *RV*s differ by 2 km s^{-1} and it may be variable.
- R105: the difference between the published *RV* (−16.0 km s^{-1}, P95) and CORAVEL data (−10.2 km s^{-1}) supports binarity.
- JJ7: there is a difference of 4 km s^{-1} between published and CORAVEL data.
- JJ27: JJ97 and present data agree on binarity.
- JJ31: large amplitude binary (JJ97 and present data).
- JJ34: binary based on all data (P95, JJ97 and present data).
- JJ36: clearly binary from CORAVEL and JJ97 data.

The cluster mean velocity, −14.63 ± 0.18 (s.e. 0.87) km s^{-1}, has been computed from 24 stars not recorded as spectroscopic binaries.

We end this section with two comments: first, the high rate of confirmed members shows that X–ray surveys are effective in detecting new cluster members, not only for very young clusters like IC 2602 and IC 2391 (e.g. Randich et al. 2001), but also for somewhat older clusters; second, whereas a detailed discussion of the evolution of rotation is beyond the scope of this paper, we note that the projected rotational velocities are rather low for the majority of the stars. More specifically, considering our sample (Table 1) and the stars from the sample of JJ97 (Table 2), there are 26 stars (∼63%) with $V \sin i \leq 10$ km s^{-1}, 13 stars (∼32%) with $10 < V \sin i \leq 20$ km s^{-1} and only 2 stars (∼5%) with $V \sin i > 20$ km s^{-1}: star R136A ($V \sin i = 26.2 \pm 2.6$ km s^{-1}) and star JJ3 ($V \sin i = 65.8 \pm 13.4$ km s^{-1}).

3.2. Abundances analysis

Effective temperatures (listed in Col. 2 of Table 3) were computed from dereddened $B-V$ colors, and using the calibration of S93: namely, $T_{\rm eff} = 1808\,(B-V)_0^2 - 6103\,(B-V)_0 + 8899$ K; we assume conservative random uncertainties $\Delta T_{\rm eff} = \pm 100$ K.

We assumed for all the sample stars the same surface gravity $\log g = 4.5$, while microturbulence was derived as

Table 2. Radial and rotational velocities and membership for part of the stars of the JJ97 sample.

No. JJ97	RV [km s^{-1}]	N	$V \sin i$ [km s^{-1}]	Spectroscopic membership (CORAVEL)
1	-15.79 ± 0.33	3	11.6 ± 1.1	M
3	-15.57 ± 2.36	2	65.8 ± 13.4	M
6	-14.49 ± 0.50	3	19.4 ± 1.2	M
7	-19.15 ± 0.45	2	12.0 ± 1.5	M, SB
8	-14.74 ± 0.54	1	4.3 ± 2.9	M
19	-12.71 ± 0.47	1	5.2 ± 3.1	M
22	-15.37 ± 0.53	3	17.3 ± 1.5	M
24	-13.24 ± 0.53	1	7.8 ± 2.9	M
27	-11.19 ± 0.59	1	15.5 ± 2.1	M, SB2
29	-13.45 ± 0.65	3	4.2 ± 1.9	M, SB?
31	$+34.44 \pm 7.37$	2	19.2 ± 1.3	M, SB
33	-14.91 ± 0.38	1	<3.2	M
34	-6.31 ± 1.96	2	6.8 ± 3.0	M, SB
36	-24.67 ± 3.24	2	12.6 ± 2.4	M, SB

$\xi = 3.2 \times 10^{-4} (T_{\rm eff} - 6390) - 1.3 (\log g - 4.16) + 1.7$ (Nissen 1981, Boesgaard & Friel 1990); these two parameters have negligible effects on Li abundances, while they affect metallicity. The assumed random errors are 0.3 dex in $\log g$ and 0.3 km s^{-1} in ξ.

3.2.1. Lithium

We carried out the Li analysis for 33 stars in our sample: star R15A was excluded since it is a doubtful member; the stars with no CORAVEL information on membership (see Table 1) were considered as possible members (M?), given their spectral characteristics and Li abundances.

We measured equivalent widths (EWs) of the Li I λ6707.8 Å doublet; at our resolutions, this spectral feature is blended, or partially blended, with the Fe I λ6707.44 Å line, therefore the contribution of the latter feature needs to be considered. The EW of the iron line was estimated following the prescription of S93, namely EW(Fe) = $[20(B-V)_0 - 3]$ mÅ. Note that the EW of star R26A ($T_{\rm eff} = 3860$ K), marked with one asterisk in Col. 3 of Table 3, has not been corrected for the Fe I contribution, since the S93 formula is no more valid for $T_{\rm eff}$ below 4000 K (see discussion in Randich et al. 2000). In this case, the quoted $\log n$(Li) should be regarded as an upper limit.

Li abundances ($\log n$(Li)) were computed from the measured EWs by interpolating the curves of growth (COG) of S93; Li abundances were then corrected for non local thermodynamic equilibrium (NLTE) effects by using the code of Carlsson et al. (1994): NLTE corrections are provided only down to $T_{\rm eff} = 4500$ K. Whereas for cooler stars we adopted LTE Li abundances, NLTE corrections are small below 4500 K (e.g. Pavlenko et al. 1995). The measured EWs of the Li+Fe feature and the EWs corrected for the Fe I blend are listed in Cols. 3 and 4 of Table 3, while the derived Li abundances are listed in Col. 5. Uncertainties in $\log n$(Li) were computed by quadratically adding the errors due to uncertainties in $T_{\rm eff}$ and in EWs.

Table 3. Li equivalent widths and Li abundances for the stars in our sample. For stars warmer than 4500 K Li abundances are corrected for NLTE effects; for the coolest stars the LTE Li abundances are reported. Star R26A, marked with an asterisk, is discussed in Sect. 3.2.1.

No. P95	$T_{\rm eff}$ [K]	EW(Li + Fe) [mÅ]	EW(Li) [mÅ]	$\log n$(Li)
R10A	4507	153 ± 5	135 ± 5	1.63 ± 0.15
R14	5888	107 ± 6	98 ± 6	2.71 ± 0.10
R16A	5656	155 ± 10	145 ± 10	2.77 ± 0.17
R26A	3860	<30*	<30	<-0.20
R27	5810	122 ± 3	113 ± 3	2.73 ± 0.10
R35	4095	73 ± 18	51 ± 18	0.28 ± 0.21
R39A	5696	108 ± 5	98 ± 5	2.56 ± 0.10
R42	6008	115 ± 4	107 ± 4	2.85 ± 0.10
R48A	4144	41 ± 10	20 ± 10	-0.12 ± 0.28
R49A	5772	92 ± 6	82 ± 6	2.53 ± 0.10
R51A	5772	46 ± 5	36 ± 5	2.13 ± 0.11
R53	5048	88 ± 12	74 ± 12	1.84 ± 0.15
R55A	5272	86 ± 10	74 ± 10	2.05 ± 0.14
R55B	6131	91 ± 3	83 ± 3	2.80 ± 0.09
R64	5622	77 ± 5	67 ± 5	2.30 ± 0.11
R66	5442	139 ± 5	128 ± 5	2.51 ± 0.11
R73A	6257	63 ± 15	56 ± 15	2.69 ± 0.17
R79A	5513	142 ± 8	131 ± 8	2.59 ± 0.12
R82	5622	128 ± 5	118 ± 5	2.61 ± 0.10
R92	5772	110 ± 5	100 ± 5	2.64 ± 0.10
R97	5772	120 ± 8	110 ± 8	2.69 ± 0.11
R102	5079	81 ± 5	67 ± 5	1.82 ± 0.13
R103	5696	111 ± 5	101 ± 5	2.58 ± 0.10
R105	5810	115 ± 3	106 ± 3	2.70 ± 0.10
R109A	5477	121 ± 7	110 ± 7	2.43 ± 0.12
R116	5110	83 ± 4	70 ± 4	1.87 ± 0.12
R123	5206	107 ± 6	94 ± 6	2.12 ± 0.12
R126A	6300	100 ± 6	93 ± 6	2.98 ± 0.09
R133	5696	145 ± 5	135 ± 5	2.76 ± 0.10
R135A	4706	170 ± 3	154 ± 3	1.76 ± 0.14
R136A	5513	108 ± 6	97 ± 6	2.41 ± 0.11
R137A	4787	156 ± 3	140 ± 3	1.79 ± 0.13
R140B	5305	105 ± 3	93 ± 3	2.20 ± 0.11

In the following, we will compare our results with those of JJ97 and J00 for NGC 6475 and with those of other clusters. In order to put all the data on a homogeneous scale, we recomputed Li abundances using the procedure described above and starting from published EWs for these clusters (NGC 6475 – JJ97 and J00; M 34 – Jones et al. 1997; Pleiades – S93 and Jones et al. 1996; and Hyades – Thorburn et al. 1993). Where necessary we also recomputed the effective temperatures (i.e. when the $T_{\rm eff}$ vs. $B-V$ calibrations used by other authors were different from the $T_{\rm eff}$ used here).

Stars, photometry, EWs and $\log n$(Li) for the samples of JJ97 and J00 are listed in Tables 4 and 5. The $T_{\rm eff}$ listed in in Tables 4 and 5 are those recomputed by us, after retrieving $B-V$ values from P95. The listed EWs were corrected for the Fe I blend by JJ97 and J00, using a spectral subtraction technique. Ten of the stars of JJ97 (marked with asterisks in Table 4) are in common with our sample: for this reason, in the

Table 4. Stellar parameters and Li abundances for the sample of JJ97. Asterisks denote stars in common with our sample. For stars warmer than 4500 K Li abundances are corrected for NLTE effects; for the coolest stars the LTE Li abundances are reported.

No. P95	No. JJ	V	$(B-V)_0$	$T_{\rm eff}$ [K]	EW(Li) [mÅ]	log n(Li)
61	1	11.58	0.62	5810	124 ± 4	2.79 ± 0.10
42	2*	11.38	0.57	6008	105 ± 9	2.84 ± 0.11
81	3	11.38	0.48	6386	58 ± 13	2.80 ± 0.15
69	4	12.13	0.60	5888	30 ± 10	2.14 ± 0.33
127B	6	11.67	0.57	6008	90 ± 14	2.75 ± 0.13
127A	7	11.88	0.61	6330	101 ± 9	3.05 ± 0.10
94	8	13.30	0.81	5142	126 ± 10	2.23 ± 0.13
82	9*	12.87	0.67	5622	127 ± 11	2.66 ± 0.12
82B	10	12.53	0.68	5585	109 ± 9	2.54 ± 0.12
53	11*	13.40	0.84	5048	68 ± 12	1.79 ± 0.16
27	12*	12.12	0.62	5810	101 ± 8	2.67 ± 0.11
16A	13*	11.69	0.66	5659	102 ± 7	2.56 ± 0.11
7B	14	13.78	1.02	4555	123 ± 17	1.62 ± 0.17
7A	15	14.15	1.00	4604	203 ± 25	2.04 ± 0.21
39A	16*	12.36	0.65	5696	134 ± 13	2.75 ± 0.13
–	17	12.30	0.69	5549	91 ± 11	2.40 ± 0.13
–	18	11.99	0.71	5477	124 ± 10	2.52 ± 0.12
76	19	13.55	0.89	4899	104 ± 11	1.88 ± 0.14
–	20	14.05	0.98	4654	59 ± 12	1.32 ± 0.17
24	22	11.11	0.44	6564	60 ± 8	2.90 ± 0.15
103	23*	12.37	0.65	5696	99 ± 12	2.57 ± 0.13
33	24	13.42	0.83	5079	127 ± 18	2.18 ± 0.16
102	25*	13.32	0.83	5079	108 ± 34	2.08 ± 0.25
14	26*	12.06	0.60	5888	97 ± 6	2.70 ± 0.10
104	27	12.37	0.76	5305	126 ± 8	2.38 ± 0.12
72	28	10.79	0.49	6343	59 ± 8	2.77 ± 0.11
95	29	12.19	0.62	5810	97 ± 8	2.64 ± 0.11
39B	31	12.19	0.63	5772	118 ± 11	2.73 ± 0.12
119A	33	12.92	0.75	5339	103 ± 9	2.29 ± 0.12
109	34	12.63	0.74	5373	90 ± 8	2.25 ± 0.13
66	35*	12.78	0.72	5442	87 ± 7	2.29 ± 0.12
132	36	11.81	0.62	5810	49 ± 14	2.29 ± 0.17
1	40	13.30	1.07	4439	17 ± 9	1.84 ± 0.31
–	41	11.57	0.52	6214	89 ± 8	2.89 ± 0.10
134	42	12.41	0.78	5239	13 ± 4	1.21 ± 0.18

first two columns of Table 4, we report both the star numbers of P95 and of JJ97, while in Table 5 only the JJ97 numbering system is adopted.

All the stars in Table 4, with the exception of JJ40, JJ41 and JJ42, were considered as bona fide cluster members (see JJ97 and Table 2). The membership of JJ40, JJ41, JJ42 requires confirmation because the available velocities are based on a single observation and differ by more than 18 km s^{-1} from the cluster mean. If members, they clearly should be binaries.

Stars in Table 5 were selected by us following the same criteria adopted by J00, i.e. stars with radial velocities far from the cluster mean velocity were rejected; since star JJ105, rejected by J00, has a RV differing only by 5 km s^{-1} from the cluster mean velocity, we consider this object as a possible member.

Table 5. Stellar parameters and Li abundances for the sample of J00. Li abundances are corrected for NLTE effects.

No. JJ	V	$(B-V)_0$	$T_{\rm eff}$ [K]	EW(Li) [mÅ]	log n(Li)
103	12.55	0.66	5658	123 ± 15	2.66 ± 0.14
104	12.18	0.72	5442	192 ± 13	2.80 ± 0.14
105	12.92	0.77	5272	34 ± 15	1.67 ± 0.25
106	12.20	0.64	5734	148 ± 11	2.84 ± 0.12
109	12.07	0.67	5622	156 ± 35	2.79 ± 0.24
110	12.96	0.80	5174	90 ± 13	2.06 ± 0.15
111	11.59	0.52	6214	132 ± 13	3.12 ± 0.12
113	11.80	0.59	5928	133 ± 17	2.92 ± 0.14
115	11.70	0.60	5888	137 ± 13	2.91 ± 0.12
116	12.29	0.64	5734	158 ± 12	2.88 ± 0.12

3.2.2. Metallicity

We used the best quality spectra to derive the cluster metallicity. The iron abundance analysis was carried out using MOOG (Sneden 1973 – version December 2000) and Kurucz (1995) model atmospheres. For each star we measured up to eight Fe I lines, whose wavelengths are listed in Table 6 (the EWs are available from S. Randich, upon request); for these lines we adjusted log gf values by carrying out an inverse abundance analysis of the solar spectrum. We used the spectrum of the Sun observed with the FEROS instrument at La Silla, during another observing run. The resolving power of the FEROS spectrum ($R \sim 48\,000$) is somewhat higher than that of our sample spectra; all the lines that we used for the iron analysis, however, do not have close features that could be blended at our resolution and that could lead to overestimate the cluster metallicity. For the Sun, we assumed log n(Fe) = 7.52 and the usual solar parameters: $T_{\rm eff\odot}$ = 5770 K, log $g_\odot$ = 4.44, and $\xi_\odot$ = 1.1 km s^{-1}. Van der Waals broadening was treated using the Unsöld approximation (1955).

The derived iron abundances for each line and the mean abundance for each star are listed in Table 6; the random errors in the mean, σ_1 and σ_2 are also listed in the table. The random errors were estimated similarly to Randich et al. (2000); namely, we assumed that, for each star, the standard deviation of the mean iron abundance would be a good estimate of the error – σ_1 – due to errors in measured EWs and to random uncertainties in atomic parameters, gf–values in particular. We then estimated random errors due to uncertainties in stellar parameters – σ_2 – by varying each parameter at a time and leaving the other two parameters unchanged; we then quadratically added the related errors. As mentioned above, conservative errors of 100 K in $T_{\rm eff}$, 0.3 dex in log g, and 0.3 km s^{-1} in ξ were assumed. Note that we did not find any abundance trend vs. EW or EP (excitation potential), meaning that our assumed parameters should not be largely in error.

In order to estimate systematic errors and to put our [Fe/H] determination for NGC 6475 on a consistent scale with other well known clusters, we determined [Fe/H] for two Hyades members. The two stars, vB182 and vB187, which have $T_{\rm eff}$ within the range covered by our sample stars, were observed by us during one observing run with UVES on VLT UT2

Table 6. Iron abundances.

Star	log n(Fe)								
	6703.57 Å	6725.36 Å	6726.67 Å	6750.16 Å	6810.27 Å	6820.37 Å	6828.60 Å	6858.15 Å	average($\pm\sigma_1 \pm \sigma_2$)
R14	–	7.87	7.61	–	7.56	7.67	7.65	7.48	$7.64 \pm 0.13 \pm 0.11$
R16A	7.64	–	7.65	7.64	7.67	7.72	7.72	7.50	$7.65 \pm 0.07 \pm 0.11$
R39A	7.65	7.76	7.66	7.57	7.52	7.64	7.61	–	$7.63 \pm 0.08 \pm 0.11$
R49A	7.62	–	–	7.55	7.89	7.56	–	7.42	$7.61 \pm 0.17 \pm 0.11$
R55A	7.68	7.80	7.66	7.75	7.68	7.73	–	7.62	$7.70 \pm 0.06 \pm 0.11$
R66	7.61	–	7.56	7.81	7.60	7.60	7.58	7.49	$7.61 \pm 0.10 \pm 0.11$
R92	7.74	–	7.68	7.78	7.67	7.69	7.66	7.53	$7.68 \pm 0.08 \pm 0.11$
R102	7.63	–	7.79	7.77	7.61	7.58	7.61	7.47	$7.64 \pm 0.11 \pm 0.14$
R103	7.69	7.64	7.83	7.59	–	7.64	7.73	7.63	$7.68 \pm 0.08 \pm 0.11$
R105	–	7.67	7.74	–	7.67	–	7.61	7.61	$7.66 \pm 0.06 \pm 0.11$
R123	7.55	–	–	7.76	–	7.70	7.68	7.67	$7.67 \pm 0.08 \pm 0.11$
vB182	7.62	7.65	7.64	7.63	–	–	–	–	$7.64 \pm 0.02 \pm 0.10$
vB187	7.66	7.67	7.68	7.64	–	–	–	–	$7.66 \pm 0.02 \pm 0.10$

(the detailed description of the data, analysis, and results will be reported elsewhere). The spectra have resolving power $R \sim 40\,000$ and S/N ratios around 200. We derived stellar parameters for the two Hyades stars consistently with our sample stars and obtained (or assumed in the case of surface gravity): $T_{\rm eff} = 5079$ K, $\log g = 4.5$, $\xi = 0.84$ km s^{-1} for vB182 and $T_{\rm eff} = 5339$ K, $\log g = 4.5$, $\xi = 0.92$ km s^{-1} for vB187. We measured the *EW*s of the four Fe I lines of the ones used by us for metallicity included in the UVES spectral range and derived iron abundances as for our sample stars. The abundances for the two Hyades stars are listed in Table 6.

We computed the weighted mean iron abundance for NGC 6475 using all the stars listed in Table 6 and obtained $\log n(\mathrm{Fe}) = 7.66 \pm 0.06$, or $[\mathrm{Fe/H}] = +0.14 \pm 0.06$. Note that, when computing the mean, we conservatively assumed for each star a total error $\sigma = \sigma_1 + \sigma_2$. The mean for the Hyades is $\log n(\mathrm{Fe}) = 7.65 \pm 0.08$ or $[\mathrm{Fe/H}] = 0.13 \pm 0.08$. In other words *a)* our metallicity for the Hyades is virtually the same as the usually quoted value for this cluster ([Fe/H] = +0.13, Boesgaard & Budge 1989), implying that our analysis should not be affected by large systematic errors; *b)* the metallicity of NGC 6475 is over–solar and very similar to that of the Hyades.

As mentioned in the introduction a metallicity larger than solar for NGC 6475 was already found by JJ97, who derived $[\mathrm{Fe/H}] = +0.11 \pm 0.034$, in good agreement with our estimate. In addition, one star in the sample of JJ97 (JJ26/R14) is in common with the sample we have used for the metallicity determination; the metallicity we derive for this star is consistent with the value quoted by JJ97 ([Fe/H] = +0.12 and +0.10, respectively). However, whereas JJ97 assumed the same $T_{\rm eff}$ values and similar $\log g$ as ours, they assumed a microturbulence $\xi = 2$ km s^{-1} for all the stars. Had we assumed this value, we would have found a much lower metallicity for the cluster ([Fe/H] ∼ solar). We note that our choice for the microturbulence parameter is more in agreement with other metallicity studies: besides Boesgaard & Friel (1990), several other authors used low, and temperature dependent, values of ξ for cluster and field dwarfs (e.g., Edvardsson et al. 1993; King et al. 2000). In addition, our microturbulence scale is consistent with the most commonly used value for the solar microturbulence which we also assumed for our inverse analysis of the solar spectrum (see above).

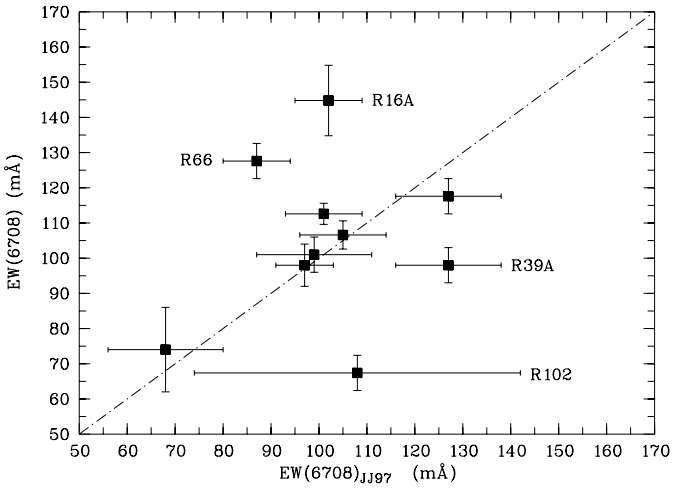

Fig. 2. Our NGC 6475 equivalent widths are plotted vs. the equivalent widths of JJ97 for the 10 stars in common.

4. Results

4.1. Lithium in NGC 6475

In Fig. 2 we plot our deblended Li *EW*s vs. the *EW*s measured by JJ97 for the ten stars in common. The figure shows a good agreement between the *EW*s of JJ97 and our measurements; however four stars are present for which the differences between the two measurements are larger than the errors: the discrepant stars are R16A and R66, for which our *EW*s are much larger than the JJ97 *EW*s, R39A and R102, which on the contrary lie well below the mean trend. The spectra of these stars (see Fig. 1) have a rather high S/N ratio and the continuum can

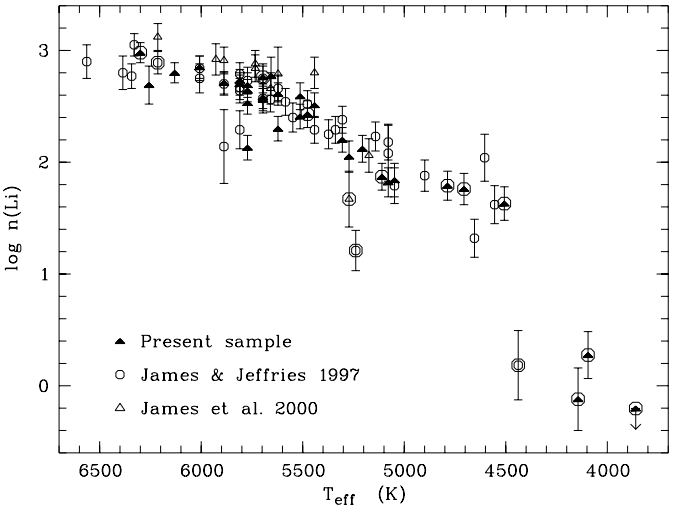

Fig. 3. NGC 6475 Li abundance vs. $T_{\rm eff}$: the present sample (filled triangles) is compared to those of JJ97 (circles) and J00 (open triangles); circled symbols denote stars whose membership is still to be confirmed, while down–pointing arrows represent upper limits in log n(Li). Error bars are also shown.

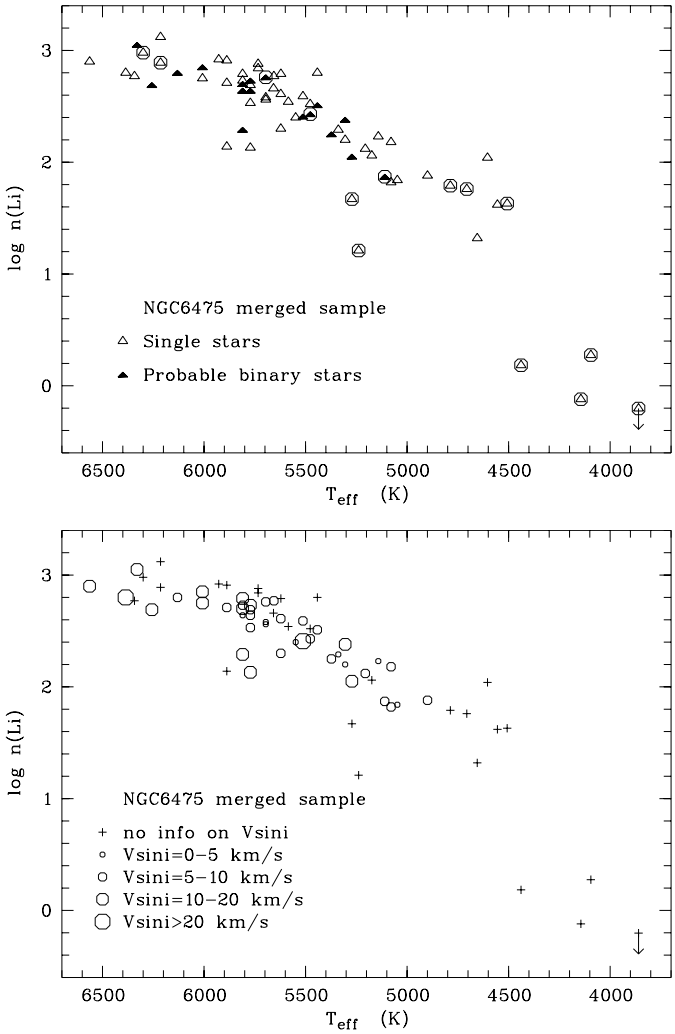

Fig. 4. Li abundance vs. $T_{\rm eff}$ for the NGC 6475 merged sample (our sample+JJ97+J00). Top panel: open triangles denote single stars, while filled triangles indicate spectroscopic binary stars. Circled symbols denote stars whose membership is still to be confirmed. Bottom panel: stars with available projected rotational velocity are plotted as open circles: the size of the circles is proportional to $V \sin i$; stars with no CORAVEL information on rotational velocity are plotted as crosses.

be clearly determined, thus an error in our EW measurements is not likely; moreover the [Fe/H] values obtained for these stars are consistent with the average estimated metallicity, which means that we have not systematically over/underestimated the EWs. Note however that star R66 is a SB2 (see Table 1): the discrepancy between the two EW measurements might be due to the fact that R66 was observed by us and JJ97 in two different phases. As far as the other three discrepant stars are concerned, whereas there is no definitive answer about the differences between the two sets of EWs, we suggest that they may be due to the different methods of subtraction of the Fe I EW (as mentioned, JJ97 used a spectral subtraction technique), or to a lower S/N of the JJ97 spectra.

The log n(Li) vs. $T_{\rm eff}$ distributions for the three samples are plotted in Fig. 3: the three distributions appear very similar; in particular no systematic difference (due, e.g., to different instruments, spectral resolutions or reduction methods) is present; the three sets therefore can be safely merged into a single larger sample. We note that the differences between our EWs and those of JJ97 for the ten stars in common are strongly reduced when considering Li abundances; in the following we will use our own Li measurements for the stars in common.

The Li vs. $T_{\rm eff}$ distribution of NGC 6475 is almost flat for the late F stars, showing little depletion with respect to the initial value (log $n(\mathrm{Li})_0$ = 3.1–3.3, as indicated from T Tauri stars and meteorites); stars with $T_{\rm eff}$ below ∼6000 K have instead undergone Li depletion with the Li distribution showing a rapid decline as the stellar temperature (mass) decreases. No evident scatter in Li abundances is present in this cluster for stars warmer than ∼4800 K, although a few stars below the mean trend are present: two of these stars have no confirmed membership (JJ42, $T_{\rm eff}$ = 5239 K and JJ105, $T_{\rm eff}$ = 5272 K), one is a probable spectroscopic binary (JJ36, $T_{\rm eff}$ = 5810 K) and two stars are confirmed as members (JJ4, $T_{\rm eff}$ = 5888 K and R51A, $T_{\rm eff}$ = 5772 K). The Li spread among cooler stars will be discussed later.

In the top panel of Fig. 4 the NGC 6475 merged sample (our stars+JJ97+J00) is shown: single and probable spectroscopic binary stars are plotted with different symbols. This plot shows that, apart from JJ36 (see above) binarity character does not alter significantly the determination of Li abundances because both kinds of stars are well mixed.

In the bottom panel of Fig. 4 NGC 6475 stars with different projected rotational velocities are represented with symbols of different size: there is no evident correlation between Li abundances and $V \sin i$ values. We stress however that, with exception of two objects with $V \sin i > 20$ km s^{-1} (see Sect. 3.1), all the other stars have low rotational velocities.

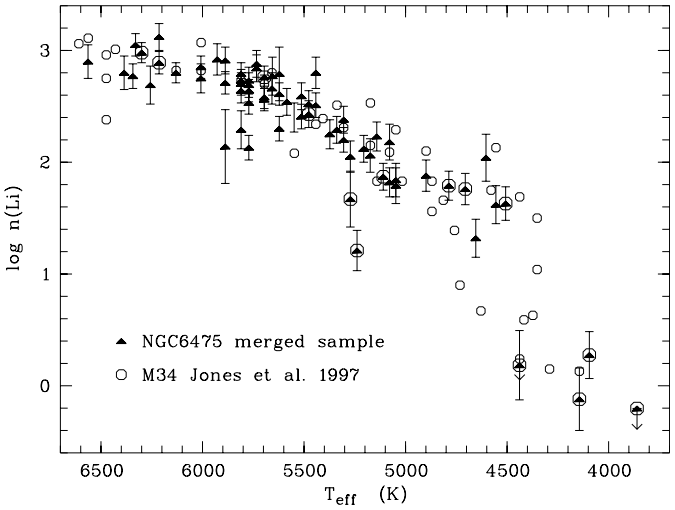

Fig. 5. Comparison of the Li distributions of the NGC 6475 merged sample (filled triangles) and M 34 (Jones et al. 1997, open circles); circled symbols denote stars whose membership is still to be confirmed.

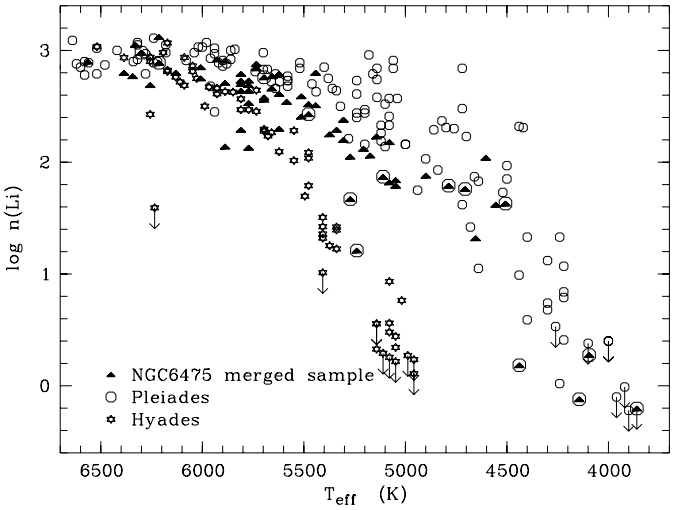

Fig. 6. The NGC 6475 Li distribution (filled triangles) is compared to those of the Pleiades (S93+Jones et al. 1996, circles) and the Hyades (Thorburn et al. 1993, stars). Circled symbols denote stars whose membership is still to be confirmed.

4.2. Comparison with other clusters

Figure 5 shows a comparison between the NGC 6475 merged sample and M 34; the two Li patterns are almost indistinguishable in spite of the slight difference in metallicity, at least down to $T_{\rm eff} \sim$ 4800–5000 K. The M 34 sample contains a significantly larger number of mid and late K–type stars than ours. An evident Li abundance star–to–star scatter is present for $T_{\rm eff} \lesssim$ 4700–4800 K; Jones et al. (1997) showed that this spread in M 34 cannot be attributed to measurement uncertainties. We have some hints of a similar scatter in NGC 6475, but our sample includes only very few stars cooler than ∼4800 K and for most of them the membership is uncertain.

In Fig. 6 we show a comparison between the Li patterns of NGC 6475, the Pleiades and the Hyades. We can divide the plot in three temperature ranges: *a)* $T_{\rm eff} \gtrsim 6000$ K: the three clusters have similar Li distributions, with a mean value slightly below the meteoritic abundance, i.e. these stars seem to suffer a very little amount of MS Li depletion. We do not consider here the Li dip observed in the Hyades stars with $T_{\rm eff} \sim 6500$ K, since our sample contains mostly stars cooler than the dip. The only Li poor star belonging to the Hyades has $T_{\rm eff} \sim 6200$ K, but its membership is uncertain and it is discussed in Thorburn et al. 1993; *b)* $5500 \lesssim T_{\rm eff} \lesssim 6000$ K: in this $T_{\rm eff}$ range, it is evident that the NGC 6475 Li pattern lies between those of the Pleiades and the Hyades, suggesting that Li depletion is a continuous process occurring for G–type stars both between ∼100 and 220 Myr and between 220 and 600 Myr. We stress that below ∼6000 K a few stars in NGC 6475 appear as depleted as (or more depleted than) the older Hyades: these stars seem to be bona fide cluster members (see Sect. 4.1) and should be further monitored; *c)* $T_{\rm eff} \lesssim 5500$ K: as well known, Pleiades stars are characterized by a large amount of scatter for late G to late K stars. The NGC 6475 distribution lies on the lower envelope of the Pleiades distribution, and several Pleiades stars exist that show the same amount of depletion as NGC 6475; the dispersion is not present in NGC 6475 at least for stars hotter than ∼4800 K: more precisely, above this temperature the only two stars that could indicate the presence of a scatter, as mentioned, are not confirmed as members; this shows that at an age of 200–250 Myr, Li abundances have already converged onto similar values. This is true also for M 34 (see Fig. 5): note that, whereas our sample for NGC 6475 is itself statistically significant for stars hotter than ∼4800 K, the two samples together allow us to exclude with an even higher significance that this result is due to low number statistics. As already evidenced, M 34 is characterized by a Li scatter among stars cooler than ∼4700–4800 K: this dispersion could be present also in NGC 6475, but the NGC 6475 sample is rather sparse in this temperature range and we cannot draw any definitive conclusion about this point.

5. Discussion

5.1. The dependence of Li depletion on metallicity

The issue of the Li–metallicity dependence has been discussed by several authors since observational results are in sharp contrast with the predictions of both standard and non–standard models. As mentioned in the introduction, the models predict that the gas opacity increases as the iron content increases: therefore, one expects the convective envelope to reach more internal layers, and Li destruction to be more efficient in higher [Fe/H] clusters. At the same time, the opacity values are also affected by the abundance of oxygen (and other α elements): in particular, an enhanced O/Fe content should move the base of the CZ towards deeper layers (Piau & Turck–Chièze 2002).

A clear effect of [Fe/H] on Li depletion has never been empirically confirmed: for example, the comparison between the Pleiades ([Fe/H] ∼ solar) and Blanco 1 ([Fe/H] = +0.14, Jeffries & James 1999), both with an age of ∼100 Myr, suggests that PMS Li depletion does not depend on metallicity.

We found NGC 6475 to have [Fe/H] = $+0.14 \pm 0.06$; as mentioned in the introduction, the metallicity of M 34 is somewhat lower, but most likely not as low as found in the early

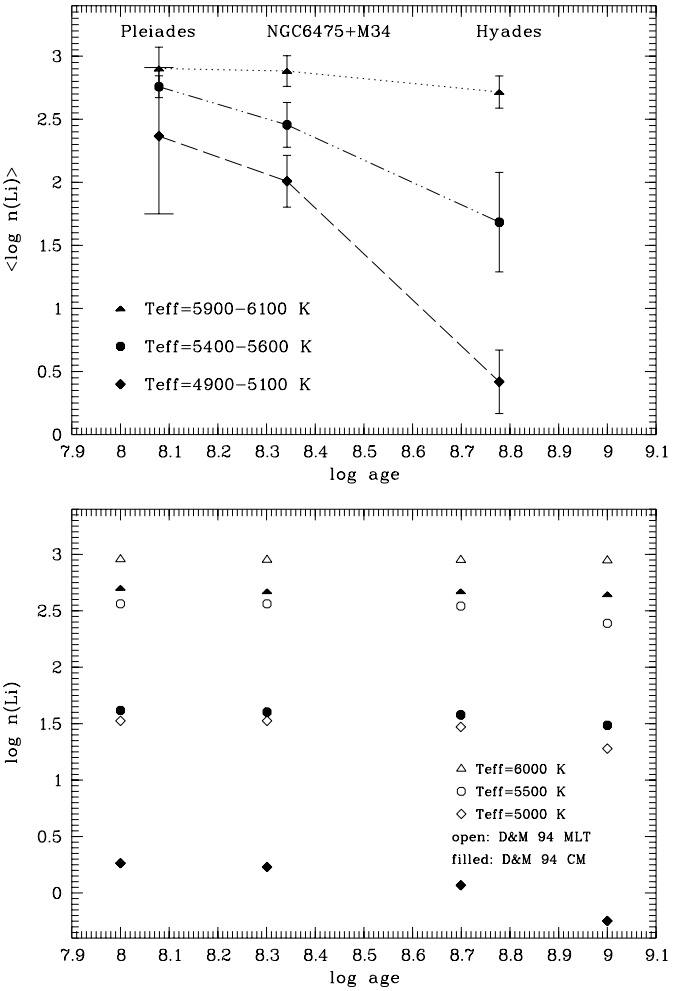

Fig. 7. Li abundance vs. log age for three ranges in $T_{\rm eff}$ (6000 ± 100 K, 5500 ± 100 K, 5000 ± 100 K). In the top panel average log n(Li) values for the Pleiades, NGC 6475+M 34 and the Hyades are shown. Error bars represent 1σ standard deviations from the average value; for the Pleiades in the range 5000 ± 100 K, where the Li spread is present, we have plotted the maximum and minimum values of log n(Li). In the bottom panel theoretical log n(Li) values at various ages are plotted (D' Antona & Mazzitelli 1994), including two different treatments of overadiabatic convection: MLT is the mixing length theory model, CM is the Canuto & Mazzitelli model.

study of Canterna et al. (1979): in fact, Schuler et al. (2003) derived for this cluster [Fe/H] = +0.07 ± 0.04. This result is based on five solar–type stars, while, considering their whole sample of nine stars with 4750 ≤ $T_{\rm eff}$ ≤ 6130 K, Schuler et al. would have derived [Fe/H] = +0.02 ± 0.02; excluding only the two coolest stars of the total sample, they would have instead found [Fe/H] = +0.04 for M 34. The value of the iron content of this cluster is a very crucial point for our discussion: as seen in Fig. 5, there are no significant differences between the log n(Li) distributions of NGC 6475 and M 34, for stars hotter than ∼4800 K. The uncertainty on the metallicity of M 34 leads to two different possibilities for the interpretation of this result: (i) if M 34 has [Fe/H] = +0.07 ± 0.04 (as probable, given the more recent and detailed analysis of Schuler et al. 2003), the similarity between the Li distribution of this cluster and NGC 6475 would not be surprising; (ii) if, on the contrary, M 34 has a lower, close to solar, metallicity, the results of Jeffries & James (1999) based on the comparison of Blanco 1 and the Pleiades would be extended to larger ages, i.e. the overall metallicity does not affect Li depletion up to the age of NGC 6475.

In any case, both possibilities allow us to safely merge the NGC 6475 and M 34 samples to investigate Li evolution as a function of age by comparing these clusters with the younger Pleiades and the older Hyades: in fact, in case (i) we can use the Pleiades in the comparison, since their Li distribution is similar to that of the over–solar metallicity Blanco 1. We will use the Pleiades instead of Blanco 1 since a very rich sample is available for the former cluster, allowing also a more detailed discussion about the spread among K–type stars; if, otherwise, case (ii) is the correct one, the Li patterns of NGC 6475 and M 34 are not affected by metallicity, thus age is the main parameter on which MS Li depletion depends. Finally and obviously, in both cases there is no problem in using the Hyades ([Fe/H] = +0.13) in our comparison.

The above discussion is valid for stars warmer than ∼4800 K; cooler stars deserve a special remark, since these stars in M 34 show a scatter in Li abundances: as mentioned, we cannot draw any definitive conclusion about the presence of a similar spread in NGC 6475. Under case (i), i.e. similar [Fe/H] for the two clusters, one would expect to find a scatter in NGC 6475. If M 34 has instead a solar metallicity (case (ii)) and the scatter exists also in NGC 6475, this would mean that the iron content does not affect Li depletion even for the coolest stars, at least at an age of ∼220–250 Myr. On the contrary, if further Li observations of NGC 6475 should demonstrate that no spread is present in this cluster, this would suggest that Li depletion in cool stars is affected by metallicity and the mechanism causing the dispersion in Li is also metal dependent.

Whereas we leave the issue of the spread among stars cooler than ∼4800 K to a future larger sample, we discuss below our results for the hotter stars.

5.2. Early–MS Li depletion

5.2.1. The observed time scales of Li depletion

The NGC 6475 merged sample confirms that MS Li depletion occurs for stars cooler than ∼6000 K, both between 120 and 220 Myr and between 220 and 600 Myr. In order to infer the time scales of Li depletion for stars of different temperatures we plot in the upper panel of Fig. 7 the average Li abundance as a function of age, for the Pleiades, the Hyades and the NGC 6475+M 34 merged sample; error bars represent 1σ standard deviations from the average values. Three different temperature ranges are considered: (i) $T_{\rm eff}$= 6000 ± 100 K, (ii) $T_{\rm eff}$ = 5500 ± 100 K, and (iii) $T_{\rm eff}$ = 5000 ± 100 K. For range (i) Li destruction occurs very slowly both between 120 and 220 Myr and between 220 and 600 Myr; in range (ii), Li depletion appears as a continuous process and it seems to be linearly related to log t, meaning that Li abundance scales as n(Li) = $t^{-\alpha}$; we found α = 1.15 in the age interval [120–220] Myr and a slightly higher slope for the

range [220–600] Myr ($\alpha = 1.77$), suggesting that Li depletion accelerates after 220 Myr. The last $T_{\rm eff}$ range is more difficult to deal with because of the presence of the Li spread for the Pleiades. First, note that for the Pleiades (in this $T_{\rm eff}$ range) the plotted error bar represents the difference between the maximum and minimum Li abundances (instead of the standard deviation). Second, if one considers the average Li abundance for stars with $T_{\rm eff}$ around 5000 K, Li destruction appears much more efficient between 220 and 600 Myr than between the age of the Pleiades and that of NGC 6475. In fact, in this case the exponents of the depletion law are $\alpha = 1.36$ ([120–220] Myr) and $\alpha = 3.65$ ([220–600] Myr), meaning that the mixing process undergoes a large acceleration for the coolest stars after ∼220 Myr. On the other hand, considering the mean log n(Li) value for Pleiades stars with $T_{\rm eff}$ around 5000 K may not be very significant, since, given the amount of scatter, the average is probably not a representative quantity. If we look instead at the evolution of Li from the maximum and minimum values in the Pleiades, up to the age of the Hyades, two different scenarios are possible: 1) Evolution from the upper envelope of the Pleiades up to the Hyades age: Li depletion occurs very rapidly and with nearly constant time scale from 120 Myr to 600 Myr; 2) Evolution from the lower envelope of the Pleiades up to the Hyades age: very little (if any) depletion occurs between ∼120 and 220 Myr, followed by a fast Li depletion between 220 Myr and the Hyades age.

5.2.2. Comparison with standard models

In order to adequately discuss these observational features, we compare the observational scenario with quantitative theoretical predictions of standard models. In the bottom panel of Fig. 7 we plot Li abundances predicted by the standard models of D' Antona & Mazzitelli (1994) for Pop. I stars ($Z = 0.019$, $Y = 0.028$) with ages ranging from 100 Myr to 1 Gyr; the three temperature ranges are the same as in the top panel of Fig. 7. Two different models are considered: in one model (MLT) the treatment of overadiabatic convection relies on the Mixing Length Theory, while the other (CM) includes the Canuto & Mazzitelli overadiabatic convection model (see D' Antona & Mazzitelli 1994 and references therein for further details). The depletion patterns are almost flat for the three temperature ranges, indicating that little depletion is expected after arrival on the ZAMS. We mention that, whereas the absolute amount of PMS depletion (and thus the value of log n(Li) at 100 Myr) depends on the treatment of overadiabatic convection, the relative amount of MS depletion which we are interested in is very small in all cases.

The comparison of the two panels of Fig. 7 shows that: (i) 6000 K– observations agree with the theoretical predictions. The models predict, during both the PMS and MS phases, a temperature at the base of the convective envelope ($T_{\rm CZ}$) which is slightly lower than (or at most similar to) the Li burning temperature ($T_{\rm Li} = 2.5 \times 10^6$ K). The agreement between observations and model predictions allows us to conclude that in late F stars no extra–mixing mechanism is probably present, at least up to the Hyades age; (ii) 5500 K – there is a clear disagreement between theory and observations: the models predict $T_{\rm CZ} \sim 3 \times 10^6$ during the PMS, but $T_{\rm CZ}$ decreases down to values around $T_{\rm Li}$ before an age of ∼100 Myr, thus very little Li depletion is present after this age[1]. Standard models cannot explain the observed MS depletion: this confirms that an extra–mixing mechanism is at work in these stars. As suggested by several authors (see Jones et al. 1997 and references therein) extra–mixing could be due to MS angular momentum loss (AML) and angular momentum transport, which, in this case should be a continuous process. If, however, Li depletion is driven by rotational mixing, it is difficult to understand the lack of dispersion among these stars which have, presumably, different rotational histories. (iii) 5000 K – during the PMS, the theoretical $T_{\rm CZ}$ is higher than the Li burning temperature, even at very young ages (∼0.3 Myr), but it decreases after arrival on ZAMS; thus, according to the models, 100 Myr old cluster stars should have depleted a large amount of Li during the PMS.

With regard to the latter point we can consider two opposite hypotheses: *a)* the upper envelope of the Pleiades is the result of PMS convection only and the lower envelope is over–depleted by the action of an extra–mixing mechanism during PMS; *b)* the lower envelope of the Pleiades is the result of convection only, while in Li rich Pleiades stars the PMS convection might have been strongly inhibited by some non–standard process; for example, as suggested by Ventura et al. (1998) and D' Antona et al. (2000), the effect of magnetic fields induced by a strong rotation could inhibit Li depletion; alternatively, a strong rotation could significantly modify the stellar structure (see Martín & Claret 1996) and prevent convection and Li depletion: both the proposed processes could explain the dispersion since both rotation and magnetic fields cover a large range of values within the same cluster (e.g. Stauffer et al. 2000).

Case *a)* appears unlikely since it would imply that, during the PMS, the convection in these cool stars "normally" do not reach deep enough layers to burn lithium. Hypothesis *b)* appears more probable; within this hypothesis one can explain both the convergence of Li abundances at the age of NGC 6475 and the large differences in Li depletion time scales in the two intervals [100–220] Myr and [220–600] Myr with the following speculative scenario: in stars of the upper envelope Li depletion is inhibited during PMS (by magnetic fields and/or rotation, see above); then, after the stars have reached the ZAMS (∼100 Myr), they start loosing angular momentum at a fast rate and extra–mixing occurs, leading to MS Li destruction which is a continuous process from 100 Myr to 600 Myr. Stars on the lower envelope (which are mostly slow rotators) during the PMS deplete a large amount of Li under the action of convection only, which stops at an age of ∼100 Myr; Li depletion becomes again sensitively efficient around the age of NGC 6475, when the decoupling between the core and the surface is large enough to have extra–mixing due to AML. Note that these cool stars have rather deep convective envelopes and

[1] We mention that, within a model, the Li burning efficiency strictly depends on the assumed nuclear reaction rates; thus, even if $T_{\rm CZ} \sim T_{\rm Li}$, the Li burning could be poorly efficient.

that during MS their T_{CZ} remains very close to the temperature which makes Li burning efficient: therefore only a small amount of extra–mixing is required for Li depletion to occur and this explains the large efficiency of Li depletion between 220 and 600 Myr, for stars of both the upper and lower envelopes.

In summary, we suggest that the spread observed among Pleiades stars cooler than ∼5500 K could be due to the fact that convection and Li depletion may be inhibited by processes related to rotation and/or magnetic fields, which vary from star to star; we also conclude that the convergence of Li abundances at the age of NGC 6475 for stars hotter than ∼4700–4800 K could be due instead to extra–mixing mechanisms, which drive the depletion after arrival on the ZAMS, and have different time scales depending on the initial rotation. Finally, we stress that in the discussion above we assumed that the spread observed in the Pleiades and M 34 is due to a real scatter in Li abundances. We mention that several authors suggested that the spread in Li equivalent widths could not necessarily correspond to a real spread in abundances, and they investigated whether the scatter could be due to the effects of surface activity (spots in particular) on the line formation and strength (e.g. Stuik et al. 1997; King et al. 2000; Randich 2001; Barrado y Navascués et al. 2001). The issue of the scatter in Li abundances remains therefore open.

6. Conclusions

We have obtained high resolution CASPEC spectra for 34 late F to K–type stars in the young open cluster NGC 6475 (age ∼220 Myr, intermediate between the Pleiades and the Hyades), thus extending the previous observations of JJ97 and J00. For a large part of the stars we derived CORAVEL information on membership and binarity: 26 stars turned out to be probable cluster members, while only one star turned out to be non–member. The other 7 stars were not observed with CORAVEL, but given their spectral characteristics and Li abundances, we considered them as probable members.

Our main results are:

a) We confirm the over–solar metallicity of the cluster; specifically we found [Fe/H] = +0.14 ± 0.06.

b) The comparison of NGC 6475 with the similar age M 34 shows no significant differences between the two Li distributions down to $T_{\rm eff} \sim 4700$–4800 K. This is not surprising, given the small difference in metallicity between the two clusters, according to Schuler et al. (2003) which found [Fe/H] = +0.07 ± 0.04 for M 34. M 34 shows an evident Li abundance spread among stars cooler than ∼4700–4800 K; the NGC 6475 sample is instead rather sparse in this temperature range. Thus, although there may be an indication for the presence of a dispersion, no definitive conclusion can be drawn. More late K–type stars in NGC 6475 should be observed.

c) Assuming that metallicity does not affect PMS Li depletion, as shown by the Pleiades–Blanco 1 comparison, we can consider the age sequence from the Pleiades, to NGC 6475+M 34 and then to the Hyades. We found that Li depletion occurs during the MS phase of G and K–type stars; the Li pattern of NGC 6475 for both G and early K stars lies between those of the Pleiades and of the Hyades. This means that extra–mixing mechanisms are likely at work both between ∼100 and ∼220 Myr and between ∼220 and ∼600 Myr.

d) The star–to–star scatter in Li abundance observed among stars cooler than ∼5500 K in clusters as young as (and younger than) the Pleiades is not present in NGC 6475 stars hotter than ∼4700–4800 K, as well as in M 34 stars over the same temperature range. We suggest that the spread observed in the Pleiades could be due to processes related to rotation and magnetic fields, which inhibit convective mixing and Li depletion during the PMS for part of the stars (those in the upper envelope); the disappearing of the scatter at the age of NGC 6475 (for stars in the temperature range [5500–4700] K) could be due to extra–mixing processes, which could also be responsible for the acceleration of Li depletion between this age and that of the Hyades.

As a final remark, we stress that the determination of oxygen and other α elements abundances are a very important issue for the investigation of Li evolution.

Acknowledgements. This work has partially been supported through a grant by Ministero dell'Istruzione, Università e Ricerca (MIUR) to S. Randich and R. Pallavicini. We thank the referee, Dr. B. F. Jones, for his very useful comments.

References

Baranne, A., Mayor, M., & Poncet, J.–L. 1979, Vistas Astron., 23, 279
Baranne, A., Queloz, D., Mayor, et al. 1996, A&AS, 119, 373
Barrado y Navascués, D., García López, R. J., Severino, G., & Gomez, M. T. 2001, A&A, 371, 652
Benz, W., & Mayor, M. 1984, A&A, 138, 183
Boesgaard, A. M., & Budge, K. G. 1989, ApJ, 338, 875
Boesgaard, A. M., & Friel, E. D. 1990, ApJ, 351, 467
Canterna, R., Perry, C. L., & Crawford, D. L. 1979, PASP, 91, 263
Carlsson, M., Rutten, R. J., Bruls, J. H. M., & Schukina, N. G. 1994, A&A, 288, 860
Chaboyer, B., Demarque, P., & Pinsonneault, M. H. 1995, ApJ, 441, 876
D' Antona, F., & Mazzitelli, I. 1994, ApJS, 90, 467
D' Antona, F., Ventura, P., & Mazzitelli, I. 2000, ApJ, 543, L77
Edvardsson, B., Andersen, J., Gustafsson, B., et al. 1993, A&A, 275, 101
García López, R. J., Rebolo, R., & Martín, E. L. 1994, A&A, 282, 518
James, D. J., & Jeffries, R. D. 1997, MNRAS, 292, 252
James, D. J., Collier Cameron, A., Barnes, J. R., & Jeffries, R. D. 2000, in Stellar Clusters and Associations: Convection, Rotation, and Dynamos, ed. R. Pallavicini, G. Micela, & S. Sciortino, ASP Conf. Ser., 198, 277
Jeffries, R. D., & James, D. J. 1999, ApJ, 511, 218
Jones, B. F., & Prosser, C. F. 1996, AJ, 111, 1193
Jones, B. F., Shetrone, M., Fisher, D., & Soderblom, D. R. 1996, AJ, 112, 186
Jones, B. F., Fischer, D., Shetrone, M., & Soderblom, D. R. 1997, AJ, 114, 352
King, J. R., Krishnamurhti, A., & Pinsonneault, M. H. 2000, AJ, 119, 859
King, J. R., Soderblom, D. R., Fisher, D., & Jones, B. F. 2000, ApJ, 533, 944
Kurucz, R. L. 1995, ApJ, 452, 102
Martín, E. L., & Claret, A. 1996, A&A, 306, 408

Martín, E. L., & Montes, D. 1997, A&A, 318, 805
Meynet, G., Mermilliod, J.-C., & Maeder, A. 1993, A&AS, 98, 477
Nissen, P. 1981, A&A, 97,145
Pallavicini, R., Cutispoto, G., Randich, S., & Gratton, R. 1993, A&A, 267, 145
Pasquini, L. 2000, in The Light Elements and their Evolution, ed. L. da Silva, M. Spite, & J. R. de Medeiros, IAU Symp., 198, 245
Pavlenko, Y. V., Rebolo, R., Martin, E. L., & García López, R. J. 1995, A&A, 303, 807
Piau, L., & Turck–Chièze, S. 2002, ApJ, 566, 419
Prosser, C. F., Stauffer, J. R., Caillault, J. P., et al. 1995, AJ, 110, 1229
Randich, S., Aharpour, N., Pallavicini, R., Prosser, C. F., & Stauffer, J. R. 1997, A&A, 323, 86
Randich, S., Martín, E. L., García López, R., & Pallavicini, R. 1998, A&A, 333, 591
Randich, S., Pasquini, L., & Pallavicini, R. 2000, A&A, 356, L25
Randich, S., Pallavicini, R., Meola, G., Stauffer, J. R., & Balachandran, S. C. 2001, A&A, 372, 862
Randich, S. 2001, A&A, 377, 512
Schuler, S., King, J. R., Fischer, D., Soderblom, D. R., & Jones, B. F. 2003, AJ, 125, 2085
Sneden, C. A. 1973, ApJ, 184, 839
Soderblom, D. R., Jones, B. F., Balachandran, S., et al. 1993, AJ, 106, 1059
Stauffer, J. R., Hartmann, L. W., Prosser, C. F., et al. 1997, ApJ, 479, 776
Stuik, R., Bruls, J. H. M. J., & Rutten, R.J . 1997, A&A, 322, 911
Swenson, F. J, Faulkner, J., Iglesias, C. A., Rogers, F. J., & Alexander, D. R. 1994, ApJ, 422, L79
Thorburn, J. A., Hobbs, L. M., Deliyannis, C. P., & Pinsonneault, M. H. 1993, ApJ, 415, 150
Udry, S., Mayor, M., & Queloz, D. 1999, in Precise Stellar Radial Velocities, IAU Coll., 170, ed. J. B. Hearnshaw, & C. D. Scarfe, ASP Conf. Ser., 185, 367
Unsöld, A. 1955, Physik der Sternatmosphären (Berlin: Springer-Verlag)
Ventura, P., Zeppieri, A., Mazzitelli, I., & D' Antona, F. 1998, A&A, 331, 1011